Twenty-six years of phytoplankton pigments reveal a circumpolar Class Divide around the Southern Ocean

Check for updates

Alexander Hayward [1,2,3] ✉, Matthew H. Pinkerton[1], Simon W. Wright[4], Andrés Gutiérrez-Rodriguez [1,5] & Cliff S. Law [1,2]

Regional taxonomic variation of phytoplankton communities in the Southern Ocean remains largely uncharacterised despite the distinct trophic and biogeochemical roles of different taxa in anthropogenic carbon uptake, biogeochemical processes, and as the primary source of energy for marine ecosystems. Here we analysed 26 years of pigment data (14,824 samples between 32°S and the Antarctic coast) from over 50 voyages (1996 – 2022), using the *phytoclass* software. The analysis confirms that the Antarctic Polar Front (APF) is a circumpolar phytoplankton class boundary, separating haptophyte dominated communities to the north from diatom domination of chlorophyll *a* in the south, and thereby a biological analogue corresponding to the Biogeochemical Divide. Furthermore, community composition was remarkably similar in different zones south of the APF despite substantial spatial variation in biomass. This circumpolar characterisation of the geospatial distribution of phytoplankton community composition will contribute to improved modelling and projection of future change in ecosystems and carbon in the Southern Ocean.

Phytoplankton stabilise Earth's climate by sequestering atmospheric carbon dioxide (CO_2) via the Biological Carbon Pump (BCP), a suite of biological and physical processes that transport photosynthetically-fixed organic matter to the deep ocean[1,2]. Phytoplankton are also the gateway for carbon and energy to enter food-webs, and are fundamental to supporting highly-productive ecosystems, for example, as the primary food source for keystone species such as Antarctic krill[3]. Both the biogeochemical and trophic roles of phytoplankton are dependent on the taxonomic community composition[4–6], and consequently, there is increasing focus on understanding how specific Southern Ocean phytoplankton groups will respond to future climate scenarios[7–11]. Advances in understanding the spatial variability in phytoplankton community composition over broad scales in the Southern Ocean are currently limited but urgently required.

The Southern Ocean is characterised by a sequence of environmentally distinct oceanographic zones (Fig. 1), distinguished by physio-chemical properties including temperature, salinity, and nutrients[12–14]. These different environmental conditions exert strong bottom-up control on phytoplankton biomass and diversity, which subsequently influence the efficiency of CO_2 sequestration and ecosystem productivity[15,16]. The most prominent hydrodynamic regional feature is the Antarctic Polar Front (APF), a

distinctive oceanographic boundary between Antarctic and Subantarctic waters[12,13]. The APF separates cold, fresh, macronutrient-rich Antarctic Surface Water (AASW), from warmer, saltier, and macronutrient rich but silicate-poor Subantarctic water (SAW)[17], with the denser AASW subducting beneath the lighter SAW[12]. The APF is recognised as a "Biogeochemical Divide"[18], characterised by discontinuity in the partial pressure of CO_2 (pCO_2) and silicate concentration between Antarctic and Subantarctic water[19,20], reflecting differences in the contributions of biological and physical mechanisms to the control of export production and air-sea CO_2 exchange[18]. These changes in physical and chemical properties also influence the biosphere, with high species level endemicity observed among many non-mammalian fauna either side of the APF[21].

These geospatial differences in biogeochemistry[18] imply a corresponding divide in phytoplankton community composition and functionality, but this has not been demonstrated empirically. In this manuscript, we reveal consistent zonal differences in phytoplankton community structure over the circumpolar Southern Ocean, based on a large dataset of phytoplankton pigments samples ($n = 14,824$) amassed over 26 years from 58 oceanographic voyages between 32°S and the Antarctic coast (see Methods). We present analysis of this pigment dataset using the

[1]National Institute of Water and Atmospheric Research, Wellington, New Zealand. [2]University Of Otago, Dunedin, New Zealand. [3]Danish Meteorological Institute, København, Denmark. [4]IMAS, University Of Tasmania, Tasmania, Australia. [5]Instituto Español de Oceanografía, Centro Oceanográfico de Gijón (IEO-CSIC), Gijón, Spain. ✉e-mail: algh@dmi.dk
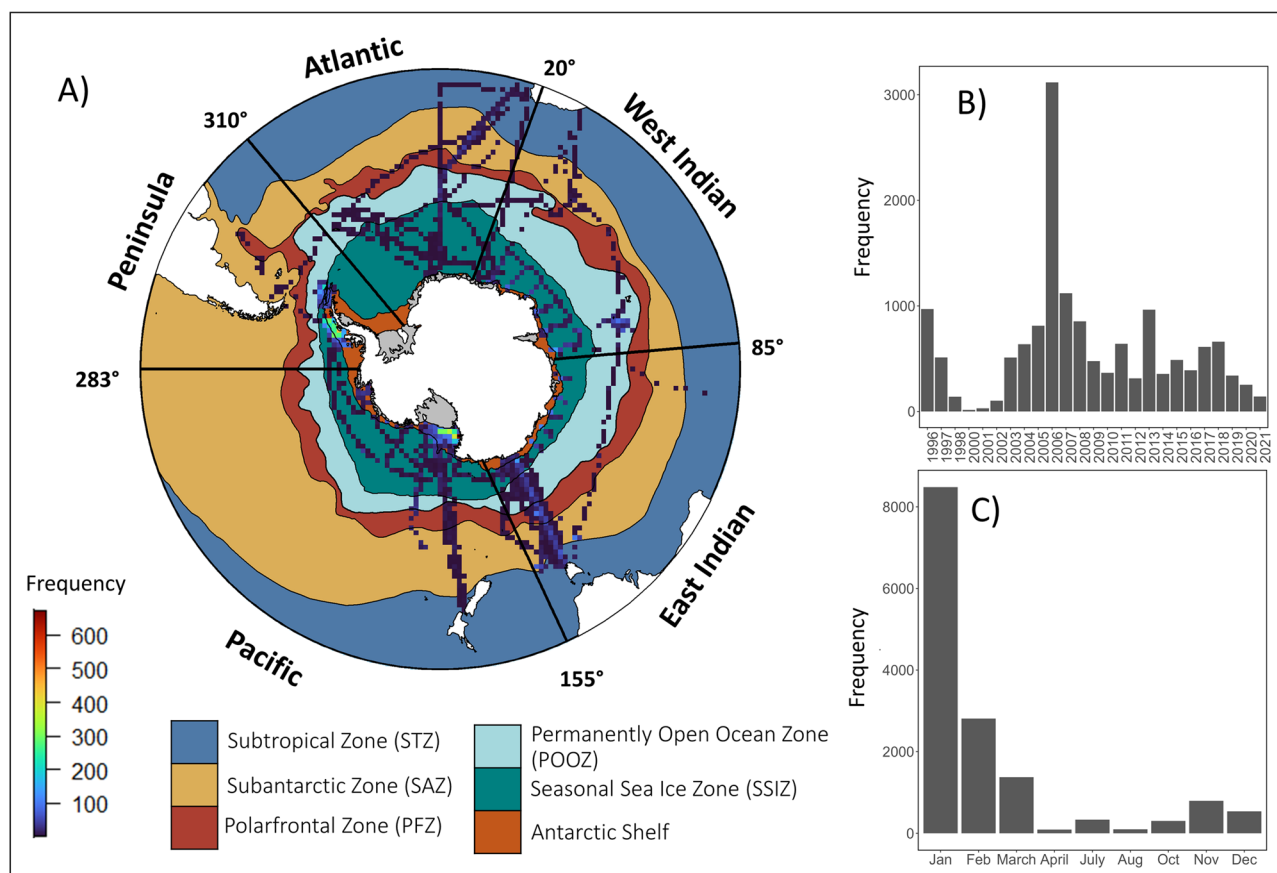
Fig. 1 | The circumpolar distribution of pigment sampling locations. Pigment distributions across the six oceanographic zones (Subtropical Zone, Subantarctic Zone, Polar Frontal Zone, Permanently Open Ocean Zone, Seasonal Sea Ice Zone, and the Antarctic Shelf; (**A**) and sampling frequency in respective years (**B**) and months (**C**). Note that the year 2006 shows an anomalously high number of samples due to two large sampling campaigns (CORSACS[49] and BROKE-West[50]).

inversion method "*phytoclass*"[22], which determined the differences in the chlorophyll *a* (Chl *a*) biomass and proportions of seven phytoplankton groups mainly at Class level (diatoms, haptophytes, cryptophytes, dino-flagellates, green algae, pelagophytes, and *Synechococcus*) across the Southern Ocean. Further, we identify the distributions of four distinct community types, revealed by cluster analysis, and show their distribution relative to the APF. The analysis identifies a phytoplankton "Class Divide" that exists as the biological analogue to the Biogeochemical Divide.

Results and Discussion
Phytoclass analysis and data distributions
The *phytoclass* software provided robust quantification of the Chl *a* biomass for phytoplankton groups estimated from the pigment data. The median root mean square error associated with each run was 0.012 mg Chl *a* m^{-3} against a median biomass of 0.42 mg Chl *a* m^{-3} and ranged from <0.01 mg Chl *a* m^{-3} to 28 mg Chl *a* m^{-3} (a coastal station in the Western Antarctic Peninsula). There were strong relationships between phytoplankton pig-ment markers and the Chl *a* biomass for each respective group (Supple-mentary Table 1).

The HPLC data used in this study provided high-quality measure-ments of Chl *a* and phytoplankton accessory pigments concentration between the Subtropics and Antarctic Shelf from 1996 to 2022, spanning the duration of the Ocean Colour satellite record, but was highly biased to the summer months (Fig. 1). The majority (85%) of samples were collected in austral summer, primarily in January (56%). Therefore, we do not report on the seasonal dynamics of phytoplankton groups; although seasonal patterns and succession are important[15,23,24], they vary regionally and are hence blurred somewhat by zonal averaging. The Antarctic Shelf region (hereafter referred as 'Shelf') was the most sampled, comprising 6,544 (44%) of total

samples, largely due to sustained long-term research efforts in the Ross Sea and Western Antarctic Peninsula (WAP). Sample size typically decreased in northerly latitudes, with the Subtropical Zone (STZ) having the fewest samples (*n* = 470).

Zonal variation of phytoplankton biomass and community composition
Figure 2 summarises phytoplankton community biomass and taxonomic composition, displaying the mean total Chl *a* (TChl *a*) biomass and phy-toplankton group proportion in each region and oceanographic zone. The mean circumpolar phytoplankton biomass across all oceanographic zones was 0.89 mg Chl *a* m^{-3}, with the highest mean biomass of 1.5 mg Chl *a* m^{-3} in the Shelf, 3 times greater than the Seasonal Sea Ice Zone (SSIZ) and Permanently Open Ocean Zone (POOZ) (0.4 and 0.5 mg Chl *a* m^{-3}, respectively; Fig. 2). North of the APF, TChl *a* in the Polar Frontal Zone (PFZ), Subantarctic Zone (SAZ) and STZ ranged between 0.4 to 0.6 mg Chl *a* m^{-3}. Averaging across all zones, diatoms were the most prevalent group with a mean biomass of 0.4 mg Chl *a* m^{-3} and mean proportion of 42% of TChl *a*, with haptophytes being the second-most abundant group with a mean biomass of 0.3 mg Chl *a* m^{-3} and 33% relative contribution (Sup-plementary Table. 3). Cryptophytes were the only other group to make a notable contribution (>10% of TChl *a*) to community biomass, although this was only in the Shelf (Supplementary Table. 2).

A clear feature of Fig. 2 is the shift in phytoplankton community composition at Class level at the APF, emphasising its role as a major boundary between diatom-dominated Antarctic zones and haptophyte-dominated sub-Antarctic zones. Although the mean TChl *a* biomass was similar either side of the APF, the community composition differed greatly (Fig. 2), with haptophytes dominating all regions of the PFZ whereas
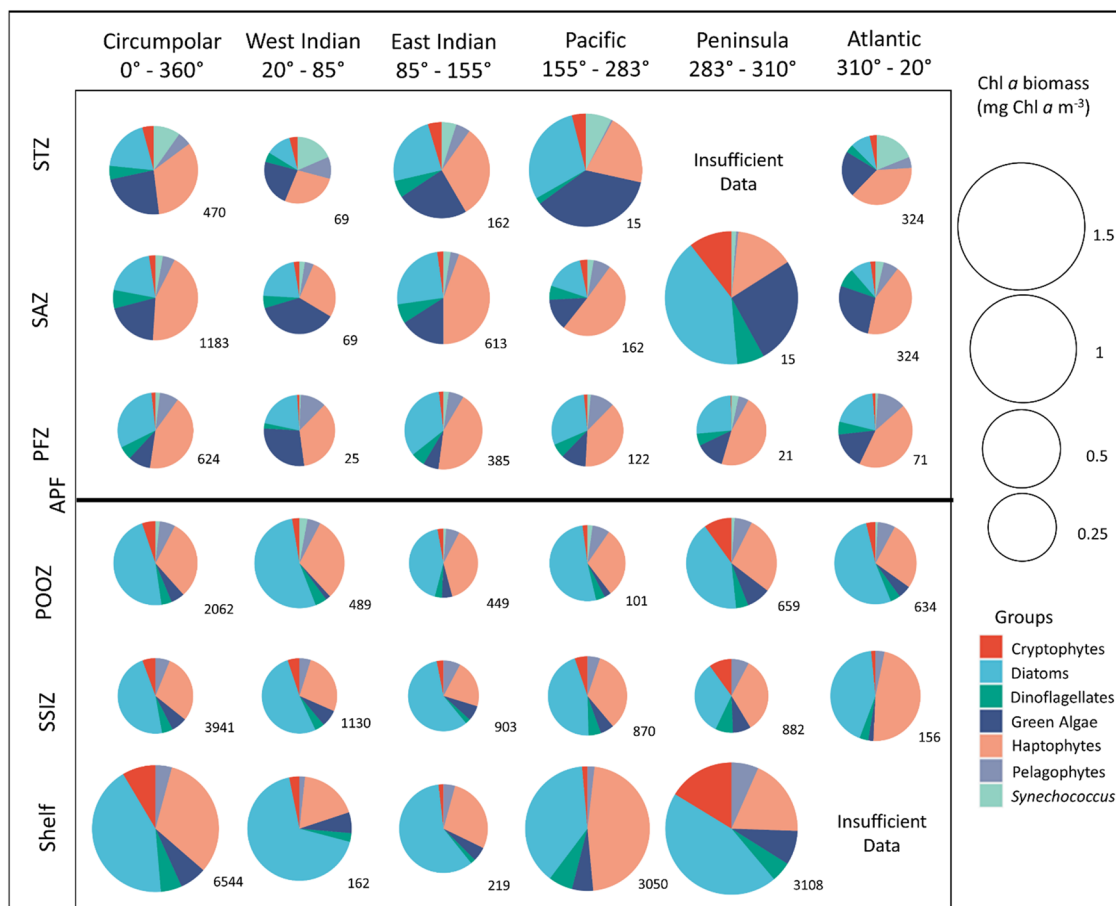
Fig. 2 | Mean proportion of the main phytoplankton groups by oceanographic zone (rows) and region (columns). The horizontal black line represents the Antarctic Polar Front (APF), where the diatom-dominated circumpolar community composition shifts to haptophyte dominance. The zones include the seasonal sea ice zone (SSIZ), the Permanently Open Ocean Zone (POOZ), the Polar Frontal Zone (PFZ); the Subantarctic Zone (SAZ) and the Subtropical Zone (STZ). The colour of the wedges indicates the phytoplankton group, and the size of the pie reflects the mean Chl *a* biomass, as identified in the keys on the right of the figure. Sample size is indicated by the number to the bottom right of each pie and "Insufficient data" indicates where sample size is less than 10.

diatoms dominated all regions in the POOZ. Furthermore, with few exceptions, the proportions of phytoplankton groups/classes in communities south of the APF were remarkably consistent, even though the total biomasses differed, whereas the relative compositions of communities north of the APF were more varied.

With respect to zonal variability, mean diatom biomass south of the APF was greatest in the Shelf region (0.7 mg Chl *a* m^{-3}), relative to the SSIZ and POOZ at 0.2 and 0.3 mg Chl *a* m^{-3}, respectively. Circumpolar dominance of diatoms was a prevalent feature of all zones south of the APF, with a mean proportion of 46%, whereas the proportion of haptophytes was lower at 32%. The only exception to this pattern was in the Pacific region where haptophytes dominated with a mean biomass of 0.75 mg Chl *a* m^{-3}, relative to 0.5 mg Chl *a* m^{-3} for diatoms, reflecting the large proportion of *Phaeocystis spp.* in the Ross Sea[25] (supplementary Table. 3). The mean proportion of flagellated groups - green algae (6%), cryptophytes (6%), and pelagophytes (5%) - was also consistent across all zones south of the APF, with slightly elevated proportion of cryptophytes (8.5%) and dinoflagellates (5%) in the Shelf region. Although community composition was consistent between zones when averaged across time and space, biomass varied greatly, signalling that environmental factors that determine community composition and biomass likely differ.

Phytoplankton community composition and biomass were also consistent across the zones to the north of the APF with respect to haptophyte dominance over diatoms, but differences emerged at the circumpolar scale, with greater variance between regions compared with south of the APF (Fig. 2). Haptophytes typically showed the highest proportion north of the

APF, with a mean contribution to TChl *a* of 40%, reflecting the dominance of coccolithophores (e.g., *E. huxleyi*)[26] that have a lower iron (Fe) requirement[19], whereas diatom growth is limited by silicate and iron[27]. The haptophyte dominance north of the APF is also consistent with the location of the Great Calcite Belt in which sub-Antarctic waters are characterised by the elevated particulate inorganic carbon and calcite synthesis of coccolithophorid haptophytes[28,29]. Conversely, south of the APF the haptophytes are primarily *Phaeocystis antarctica*, a species which exists in both solitary and colonial forms, that has greater Fe requirement than coccolithophores[30,31]. In addition, green algae were an important component north of the APF, with a greater mean proportion than diatoms, and were occasionally dominant in regions of the STZ and SAZ, where they reached a maximum of 24%. *Synechococcus* were more prevalent north of the APF with the highest biomass (0.04 mg Chl *a* m^{-3}) in the warmer STZ accounting for 10% of TChl *a*.

The 26 years of pigment data revealed the presence of a north-south Class Divide at the APF between haptophyte dominance and higher green algae biomass to the north, and diatom dominance to the south. Regionally constrained Southern Ocean pigment studies on phytoplankton communities typically show agreement with this study. For example, over a latitudinal transect between the Antarctic and Equatorial Pacific, DiTullio et al.[32] showed negligible diatom biomass between the APF and STF[32], concurrent with diminished silicate concentrations; pelagophyte and haptophyte biomass on the other hand were elevated. Pigment-based studies, such as Schlüter et al.[33], have also confirmed higher biomass of coccolithophores (such as *E. huxleyi*) type haptophytes in the Subantarctic[33].

In higher latitudes, other studies have also observed haptophyte dominance in the Ross Sea[25,34,35] and higher proportions of cryptophytes in the WAP have previously been identified through pigment analysis[36]. Although our dataset indicates haptophyte (*Phaeocystis* Spp.) dominance in the Ross Sea, this region regularly harbours large diatom blooms, especially around Terra Nova Bay[34,37], which is also reflected in our dataset. Although there are clear similarities between this study and others, we acknowledge that any seasonal succession such as the transition of haptophytes to diatoms from spring to summer[15], will not be apparent in this analysis.

Cluster analysis identifies regional community distributions

Cluster analysis of the proportion of phytoplankton groups in each sample revealed four different community types (supplementary Table. 4) – a haptophyte-dominated community (cluster-H), a mixed community co-dominated by diatoms and haptophytes, with greater proportions of flagellates (cluster-M), a diatom-dominated community (cluster-D), and a community primarily comprised of haptophytes and green algae (cluster-HG). Clusters were derived using hierarchical clustering techniques on the proportions of phytoplankton classes and the DynamicTreeCut package[38] was used to prune dendrogram branches (see Methods). Despite no a priori information on the geographical coordinates in the analysis, clear spatial patterns emerged either side of the APF (Fig. 3). Clusters-H, M and D were predominantly located south of the APF, with only a few samples to the north (Supplementary Table. 4), whereas cluster-HG only contained samples from north of the APF. In zones south of the APF, there did not appear to be any association between specific clusters and geographical location (Fig. 3), apart from clear regional differences between the Ross Sea and the WAP. In the Ross Sea, there was higher density of cluster-H samples near the Ross Ice Shelf while cluster-D were located mainly around Terra Nova Bay; conversely there was a higher density of cluster-M and cluster-D in the WAP but no clear spatial patterns in their relative distributions.

All clusters reflect a mix of phytoplankton groups, and as such, are not directly comparable to the proportion of phytoplankton groups displayed in

Fig. 2. Yet the Class Divide between characteristic phytoplankton communities at the APF also separated cluster-HG north of the APF from the other clusters south of the APF. The overlapping distribution of clusters H, M and D south of the APF was consistent with the similarity in mean proportion of phytoplankton classes across zones (i.e., no cluster was found solely within a particular zone).

The identified Class Divide provides a biological analogue to the well-known discontinuity in environmental variables "the Biogeochemical Divide"[18], demonstrating the role of phytoplankton community composition in nutrient cycling and fate of carbon either side of the APF. These findings also highlight the importance of physico-chemical factors that shape phytoplankton communities as differences in nutrient and environmental conditions are large at this divide[18–20].

Many modelling studies and experiments have investigated how taxonomic groups will respond to a changing climate, and in turn how this will affect food-web dynamics and biogeochemical cycles[2,39]. Given the pressing need to understand spatial patterns in phytoplankton community structure, and how they relate to environmental parameters, the results presented here represent a substantial advance in characterising the distribution of phytoplankton groups throughout the Southern Ocean. Our results highlight the importance of incorporating phytoplankton community composition in ocean biogeochemical and earth system models. Recognition of the Class Divide and associated community consistency either side of the APF, and adoption of the cluster analysis to reduce the dimensionality of phytoplankton diversity, would simplify representation of phytoplankton groups in models and future projections of the Southern Ocean.

Methods
Geographical scope
Phytoplankton pigment data from 58 voyages between 1996 – 2022 were acquired from personal correspondence with scientists, publicly available repositories, and voyages associated with publications (Supplementary Table. 5).
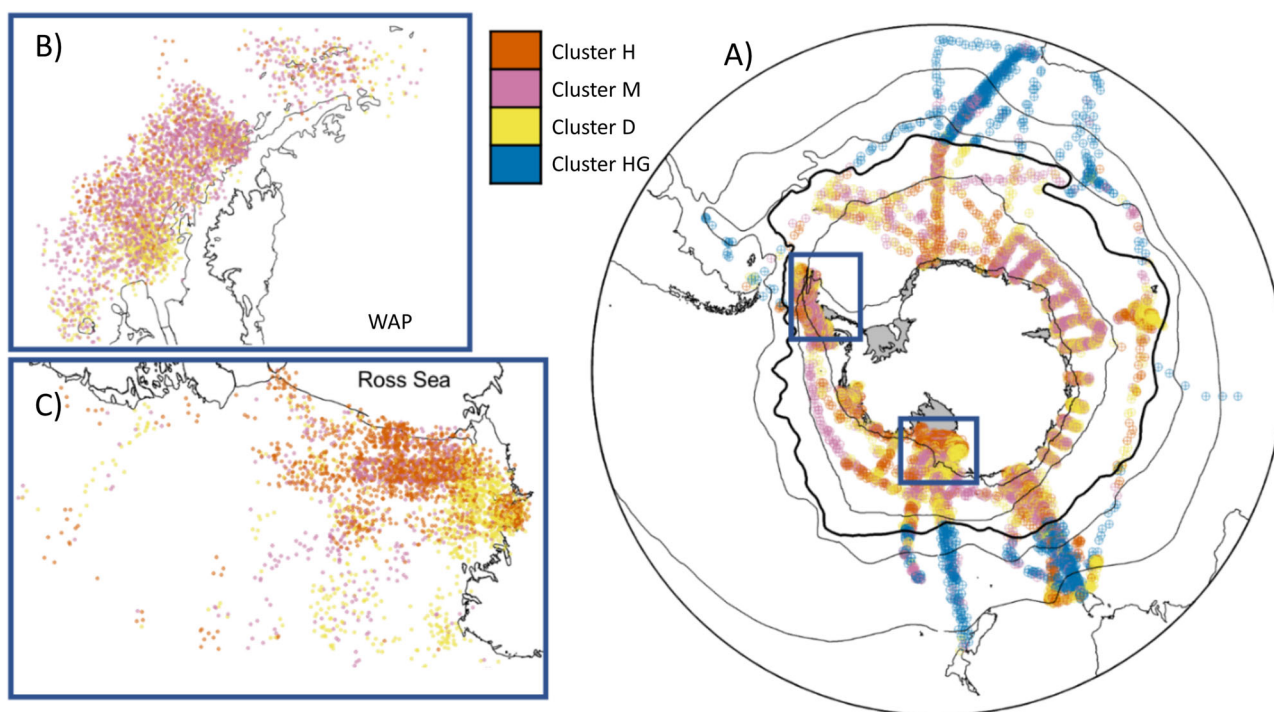

Fig. 3 | Circumpolar distribution of phytoplankton community types derived from cluster analysis. A represents cluster distributions on a circumpolar scale, **B** is within the Western Antarctic Peninsula and **C** is in the Ross Sea. Cluster-H represents haptophyte domination, Cluster-M represents a mixed community, Cluster-D represents diatom domination, and Cluster-HG represents co-domination by haptophytes and green algae. Some samples have been spatially displaced to limit overlap of samples taken at a similar location. The Antarctic Polar Front is depicted by the bold line.

To ensure consistency amongst major algal taxa, only pigment samples with all the following pigments were considered for analysis: Fucoxanthin (Fuco), 19'-Butanoyloxyfucoxanthin (But), 19'-Hexanoyloxyfucoxanthin (Hex), Chlorophyll *b* (Chl *b*), Zeaxanthin (Zea), Peridinin (Per), Prasinoxanthin (Pras), Alloxanthin (Allo), and Chlorophyll *a* (Chl *a*). This eliminated many of the pigment samples associated with the Palmer Long Term Ecological Research Centre, data prior to 1995, and much of the data in the MAREDAT database (Peloquin et al., 2013). Dependent upon availability, the following pigments were also considered: Neoxanthin (Neo), Lutein (Lut), Violaxanthin (Viol), Chlorophyll c2 monogalactosyldiacylglyceride ester Chl c2-MGDG [14:0/14:0] from *Chrysochromulina polylepis*, (MDGD-14), Chlorophyll c2 monogalactosyldiacylglyceride ester Chl c2-MGDG [18:4/14:0] from *Emiliania huxleyi* (MDGD-18). The pigment data then underwent quality control with data omitted if Chl *a* concentration was zero. Further to this, the distributions of pigments were inspected for outliers by examining frequency distributions; if present they were examined relative to other pigments at the sampling location and, if spurious, omitted from the dataset. Spatial co-ordinates and dates were also analysed to ensure format homogeneity.

Phytoclass inversion

Prior to inversion, the pigment samples were geospatially divided into the oceanographic zones listed above, using the analysis package "SF" in the programming language "R"[40]. As sea surface height (SSH) contours determined from remote sensing products do not correspond to the position of oceanographic fronts, there is currently little evidence of recent meridional frontal migration[41], and so our zonal division of the samples was based on the static frontal boundaries defined by Orsi et al.[12], which include the STF, SAF, and APF[12]. The American National Snow and Ice Data Centre (NSIDC) baseline median value of the maximum winter sea-ice extent between (1991 – 2020)[42] was used to determine the boundary of the SSIZ. To further divide samples from the Antarctic continental shelf, we used the bathymetry data of Amblas et al., (2018) for the Antarctic shelf break[43].

Prior to analysis, samples were hierarchically clustered based on their pigment to chlorophyll *a* ratios. First, pigment samples with zero concentration were imputed to 0.1% of their minimum concentrations to allow for the division by Chl *a*. Pigment ratios were then transformed using the Box-Cox method[44]. Manhattan distances were calculated between the standardised pigment ratios and then clustered using the Ward method[45] to account for the high dimensionality of the pigment data, and to identify outliers. The dynamcTreeCuti R- package[38] was used to determine the height at which to cut the dendrogram. This method allows for dynamic pruning of dendrogram branches based on their significance and has been proven effective at clustering potential outliers[38]. A minimum cluster size was set to 13 to account for sensitivity to sample sizes, as suggested by Hayward et al., 2023[22]. The samples split into 720 clusters, which were inverted to phytoplankton groups using the *phytoclass* program[22].

The *phytoclass* program is an inversion tool that uses the diagnostic marker pigments within phytoplankton groups to estimate their contribution to total chlorophyll *a* biomass. The method inverts mass concentrations of phytoplankton pigments into predefined phytoplankton groups and returns the biomass of each group in units of chlorophyll *a* concentration. This approach is similar to the widely used CHEMTAX method[46], as both address the problem that diagnostic pigments may be shared between taxa with unknown ratios, however, *phytoclass* has higher accuracy[22] and can be implemented on a large number of datasets. The *phytoclass* software was set with an iteration count of 1000 and a step of 0.006, increasing the probability of the algorithm finding the global minimum of the solution space.

The following phytoplankton groups were considered in the analysis: diatoms, haptophytes, cryptophytes, dinoflagellates, green algae, pelagophytes, and *Synechococcus*. To maintain a low condition number (i.e., ensure that the matrix inversion has a solution), and improve the accuracy of the matrix inversion, we opted for simplicity in the set-up of the *phytoclass*

analysis, by omitting haptophyte subgroups. If a major diagnostic pigment was absent from a cluster, then the relevant phytoplankton group would be omitted from the analysis, as for example, with chlorophyll *b* and the green algae lineage. Due to the latitudinal dependence and thermal threshold of *Synechococcus* in the Southern Ocean[47], and its potential mismatch with flavobacteria[48], this group was omitted from analysis in the Shelf and SSIZ regions. As most pigment samples did not contain the 'gyroxanthin' pigment, dinoflagellate type-2 (e.g., *Karenia* species) were also omitted.

To ensure the program adequately fit phytoplankton groups to their respective pigments, the root mean square error (RMSE) was assessed for each cluster and pigment-to-chlorophyll *a* ratios were also inspected for outliers. If outliers were present, or at the border of their limits, as defined in the literature, the cluster was inspected and reanalysed with the removal of an outlying pigment. Regression and multiple linear regression analysis were then performed between phytoplankton groups and their respective pigment concentrations, to ensure no non-linear relationships between pigments and phytoplankton groups were present.

Cluster analysis

Following the inversion of pigments into respective biomasses for phytoplankton groups, samples were then divided by total chlorophyll *a* to determine the relative contribution of each group to community biomass. Phytoplankton proportions were Box-Cox transformed and then Euclidean distances between the relative biomass of phytoplankton groups were generated by applying the "DynamicCutTree" package. This method pruned the hierarchical dendrogram at sensible heights, with a minimum sample size of 1000 to ensure a manageable number of clusters[38].

Reporting summary

Data availability

All data on phytoplankton pigments and the chlorophyll *a* concentrations of each phytoplankton group has been made available to the following Github repository: https://github.com/AlexiHayw/NComms_data.

References

1. Basu, S. & Mackey, K. R. Phytoplankton as key mediators of the biological carbon pump: Their responses to a changing climate. *Sustainability* **10**, 869 (2018).
2. Boyd, P. W. Physiology and iron modulate diverse responses of diatoms to a warming Southern Ocean. *Nat. Clim. Chan.* **9**, 148–152 (2019).
3. Haberman, K. L., Ross, R. M. & Quetin, L. B. Diet of the Antarctic krill (Euphausia superba Dana): II. Selective grazing in mixed phytoplankton assemblages. *J. Exp. Marine Biol. Ecol.* **283**, 97–113 (2003).
4. Vanni, M. J. & Findlay, D. L. Trophic cascades and phytoplankton community structure. *Ecology.* **71**, 921–937 (1990).
5. Le Quere, C. et al. Ecosystem dynamics based on plankton functional types for global ocean biogeochemistry models. *Global Chan. Biol.* **11**, 2016–2040 (2005).
6. Tréguer, P. et al. Influence of diatom diversity on the ocean biological carbon pump. *Nat. Geosci.* **11**, 27–37 (2018).
7. Boyd, P. W., Strzepek, R., Fu, F. & Hutchins, D. A. Environmental control of open-ocean phytoplankton groups: Now and in the future. *Limnol. Oceanograp.* **55**, 1353–1376 (2010).
8. Lassen, M. K., Nielsen, K. D., Richardson, K., Garde, K. & Schlüter, L. The effects of temperature increases on a temperate phytoplankton community—a mesocosm climate change scenario. *J. Exp. Biol. Ecol.* **383**, 79–88 (2010).
9. Petrou, K. et al. Southern Ocean phytoplankton physiology in a changing climate. *J. Plant Physiol.* **203**, 135–150 (2016).

10. Henson, S. A., Cael, B. B., Allen, S. R. & Dutkiewicz, S. Future phytoplankton diversity in a changing climate. *Nat. Commun.* **12**, 5372 (2021).

11. Ban, Z., Hu, X. & Li, J. Tipping points of marine phytoplankton to multiple environmental stressors. *Nat. Clim. Chan.* **12**, 1045–1051 (2022).

12. Orsi, A. H., Whitworth, T. I. I. I. & Nowlin, W. D. Jr On the meridional extent and fronts of the Antarctic Circumpolar Current. *Deep Sea Res. Part I: Oceanograp. Res. Papers* **42**, 641–673 (1995).

13. Sokolov, S., & Rintoul, S. R. Circumpolar structure and distribution of the Antarctic Circumpolar Current fronts: 1. Mean circumpolar paths. *J. Geophys. Res.: Oceans*, **114** https://doi.org/10.1029/2008JC005108 (2009).

14. Deppeler, S. L. & Davidson, A. T. Southern Ocean phytoplankton in a changing climate. *Front. Marine Sci.* **4**, 40 (2017).

15. Smith, W. O. Jr, Ainley, D. G., Arrigo, K. R. & Dinniman, M. S. The oceanography and ecology of the Ross Sea. *Ann. Rev. Marine Sci.* **6**, 469–487 (2014).

16. Henley, S. F. et al. Changing biogeochemistry of the Southern Ocean and its ecosystem implications. *Front. Marine Sci.* **7**, 581 (2020).

17. Freeman, N. M., Lovenduski, N. S. & Gent, P. R. Temporal variability in the Antarctic polar front (2002–2014). *J. Geophys. Res.: Oceans* **121**, 7263–7276 (2016).

18. Marinov, I., Gnanadesikan, A., Toggweiler, J. R. & Sarmiento, J. L. The southern ocean biogeochemical divide. *Nature* **441**, 964–967 (2006).

19. Nissen, C., Vogt, M., Münnich, M., Gruber, N. & Haumann, F. A. Factors controlling coccolithophore biogeography in the Southern Ocean. *Biogeosciences* **15**, 6997–7024 (2018).

20. Freeman, N. M. et al. The variable and changing Southern Ocean silicate front: insights from the CESM Large Ensemble. *Global Biogeochem. Cycles* **32**, 752–768 (2018).

21. Clarke, A., Barnes, D. K. & Hodgson, D. A. How isolated is Antarctica? *Trend Ecol. Evol.* **20**, 1–3 (2005).

22. Hayward, A. G., Pinkerton, M. H. & Gutierrez-Rodriguez, A. G. Phytoclass: A pigment-based chemotaxonomic method to determine the biomass of phytoplankton classes. *Limnol Oceanograp –* Methods, https://doi.org/10.1002/lom3.10541 (2023).

23. Arteaga, L. A., Boss, E., Behrenfeld, M. J., Westberry, T. K. & Sarmiento, J. L. Seasonal modulation of phytoplankton biomass in the Southern Ocean. *Nat. Commun.* **11**, 5364 (2020).

24. Thomalla, S. J. et al. Southern Ocean phytoplankton dynamics and carbon export: insights from a seasonal cycle approach. *Philosoph. Trans. Royal Soc. A* **381**, 20220068 (2023).

25. DiTullio, G. R. & Smith, W. O. Jr Spatial patterns in phytoplankton biomass and pigment distributions in the Ross Sea. *J. Geophys. Res.: Oceans* **101**, 18467–18477 (1996).

26. Holligan, P. M., Charalampopoulou, A., & Hutson, R. Seasonal distributions of the coccolithophore, Emiliania huxleyi, and of particulate inorganic carbon in surface waters of the Scotia Sea. *Journal of Marine Systems*. **82**, 195–205 (2010).

27. Moore, J. K. & Abbott, M. R. Surface chlorophyll concentrations in relation to the Antarctic Polar Front: seasonal and spatial patterns from satellite observations. *J. Marine Syst.* **37**, 69–86 (2002).

28. Balch, W. M. et al. Factors regulating the Great Calcite Belt in the Southern Ocean and its biogeochemical significance. *Global Biogeochem. Cycles* **30**, 1124–1144 (2016).

29. Balch W. M. et al. The contribution of coccolithophores to the optical and inorganic carbon budgets during the Southern Ocean Gas Exchange Experiment: New evidence in support of the "Great Calcite Belt" hypothesis. *J. Geophys. Res: Oceans*. **116**, https://doi.org/10.1029/2011JC006941 (2011).

30. Weisse, T., Tande, K., Verity, P., Hansen, F. & Gieskes, W. The trophic significance of Phaeocystis blooms. *J. Marine Syst.* **5**, 67–79 (1994).

31. Smith, W. O. Jr, & Trimborn, S. Phaeocystis: A global enigma. *Ann. Rev. Marine Sci.* 16. https://doi.org/10.1146/annurev-marine-022223-025031 (2023).

32. DiTullio, G. R. et al. Phytoplankton assemblage structure and primary productivity along 170 W in the South Pacific Ocean. *Marine Ecol. Progress Series* **255**, 55–80 (2003).

33. Schlüter, L., Henriksen, P., Nielsen, T. G. & Jakobsen, H. H. Phytoplankton composition and biomass across the southern Indian Ocean. *Deep Sea Res. Part I: Oceanograp. Res. Papers* **58**, 546–556 (2011).

34. Arrigo, K. R., Weiss, A. M. & Smith, W. O. Jr Physical forcing of phytoplankton dynamics in the southwestern Ross Sea. *J. Geophys. Res.: Oceans* **103**, 1007–1021 (1998).

35. Mangoni, O. et al. Phaeocystis antarctica unusual summer bloom in stratified antarctic coastal waters (Terra Nova Bay, Ross Sea). *Marine Environ. Res.* **151**, 104733 (2019).

36. Nunes, S. et al. Phytoplankton community structure in contrasting ecosystems of the Southern Ocean: South Georgia, South Orkneys and western Antarctic Peninsula. *Deep Sea Res. Part I: Oceanograp. Res. Papers* **151**, 103059 (2019).

37. Leventer, A. & Dunbar, R. B. Factors influencing the distribution of diatoms and other algae in the Ross Sea. *J. Geophys. Res.: Oceans* **101**, 18489–18500 (1996).

38. Langfelder, P., Zhang, B. & Horvath, S. Defining clusters from a hierarchical cluster tree: the Dynamic Tree Cut package for R. *Bioinformatics* **24**, 719–720 (2008).

39. Pinkerton, M. H. et al. Evidence for the impact of climate change on primary producers in the Southern Ocean. *Front. Ecol. Evol.* **9**, 592027 (2021).

40. Pebesma E. J. Simple features for R: standardized support for spatial vector data. *R J.* **10**, 439 (2018).

41. Chapman, C. C. New perspectives on frontal variability in the Southern Ocean. *J. Phys. Oceanograp.* **47**, 1151–1168 (2017).

42. Peng, G., Meier, W. N., Scott, D. J. & Savoie, M. H. A long-term and reproducible passive microwave sea ice concentration data record for climate studies and monitoring. *Earth Syst. Sci. Data* **5**, 311–318 (2013).

43. Amblas, D. & Dowdeswell, J. A. Physiographic influences on dense shelf-water cascading down the Antarctic continental slope. *Earth-Sci. Rev.* **185**, 887–900 (2018).

44. Sakia, R. M. The Box-Cox transformation technique: a review. *J. Royal Stat Society: Series D (Statistician)* **41**, 169–178 (1992).

45. Murtagh F., Legendre P. 2014. Ward's hierarchical agglomerative clustering method: which algorithms implement Ward's criterion? *J. Classificat.* 274–295 (2018).

46. Mackey, M. D., Mackey, D. J., Higgins, H. W. & Wright, S. W. CHEMTAX-a program for estimating class abundances from chemical markers: application to HPLC measurements of phytoplankton. *Marine Ecol. Progress Series* **144**, 265–283 (1996).

47. Pittera, J. et al. Connecting thermal physiology and latitudinal niche partitioning in marine Synechococcus. *ISME J* **8**, 1221–1236 (2014).

48. Alcantara, S. & Sanchez, S. Influence of carbon and nitrogen sources on Flavobacterium growth and zeaxanthin biosynthesis. *J. Indust. Microbiol. Biotechnol.* **23**, 697–700 (1999).

49. DiTullio, G. Algal pigment concentrations as measured by HPLC from RVIB Nathaniel B. Palmer cruises in the Ross Sea Southern Ocean from 2005 to 2006 (CORSACS project). Biological and Chemical Oceanography Data Management Office (BCO-DMO). (Version 08 September 2010) Version Date 2010-09-08 [if applicable, indicate subset used]. http://lod.bco-dmo.org/id/dataset/3360. (2010) [access date].

50. Wright, S. W. et al. Phytoplankton community structure and stocks in the Southern Ocean (30–80 E) determined by CHEMTAX analysis of HPLC pigment signatures. *Deep Sea ResPart II Topical Stud Oceanograp* **57**, 758–778 (2010).

Acknowledgements

Author contributions

Data Analysis: Alexander Hayward, Matt Pinkerton, Simon Wright. Conception and design: Alexander Hayward, Matt Pinkerton, Simon Wright, Andrés Gutiérrez-Rodriguez, Cliff Law. Manuscript Drafting and writing: Alexander Hayward, Matt Pinkerton, Simon Wright, Andrés Gutiérrez-Rodriguez, Cliff Law.

Competing interests

The authors declare no competing interests.

Additional information

Supplementary information The online version contains supplementary material available at https://doi.org/10.1038/s43247-024-01261-6.

Correspondence and requests for materials should be addressed to Alexander Hayward.

Peer review information *Communications Earth & Environment* thanks Alex Poulton, Marta Estrada and the other, anonymous, reviewer(s) for their contribution to the peer review of this work. Primary Handling Editors: Ilka Peeken and Clare Davis. A peer review file is available.

Reprints and permissions information is available at http://www.nature.com/reprints

Publisher's note Springer Nature remains neutral with regard to jurisdictional claims in published maps and institutional affiliations.